Experiments in Fluids 28 (2000) 377–384 © Springer-Verlag 2000

Design of air curtains used for area confinement in tunnels

L. Guyonnaud, C. Solliec, M. Dufresne de Virel, C. Rey

Abstract Air curtains' devices, i.e., plane air jets, are used as virtual screens to reduce the heat and mass transfer from one zone to another subjected to different environmental or climatic conditions. An air curtain is a plane air jet blown through an opening. It produces a pressure drop that forbids transversal flow through the opening. The principal advantage of such installations is to facilitate the transit of people, vehicles or material through doorways of buildings and other enclosures. The purpose of this research is twofold: (i) to characterize the efficiency of air curtains; (ii) to establish how scaled down models could be used to set up full-scale installations.

List of symbols

C_1,C_2	constants
e	air curtain thickness
Eu	Euler number
H	roof height
I_0	turbulence intensity of the jet at nozzle
k	constant
P_A	atmospheric pressure
P_1	static pressure in the upstream section
P_2	static pressure in the downstream section
R	jet bending radius
Re	Reynolds number of the jet at nozzle
Sc	scale of the mode
$U(x,y)$	velocity at x,y location
$U_C(x)$	centerline velocity at x location
U_0	velocity of the jet at nozzle
U_1	flow rate velocity in the main tunnel
x,y	coordinates

Greek symbols

$\Delta P = P_1 - P_2$	pressure drop created by the air curtain
ν	kinematic viscosity of air
ρ	air density
α	blowing angle
σ_1, σ_2	constants

Received: 15 October 1998/Accepted: 30 June 1999

L. Guyonnaud[1], C. Solliec
Ecole des Mines de Nantes, 4 rue A. Kastler,
F-44 307, Nantes, France

M. Dufresne de Virel
Centre Scientifique et Technique du Bâtiment,
11, rue H. Picherit,
F-44 300 Nantes – France

C. Rey
I.R.P.H.E – U.M.R 6594 C.N.R.S
Technopole de château Gombert
33, rue F. Joliot Curie,
F-13 451 Marseille, cedex 10 – France

Present address:
[1] Commissariat à l'Energie Atomique, Grenoble, France

Correspondence to: C. Solliec

We thank Miss Y. Herlédant for her reading and the Scientific and Technological Center for Buildings of Nantes – France, for its active scientific collaboration and financial support.

1 Introduction

Most of the time, traditional door causes unacceptable hindering of traffic, transport or execution of technological processes. To facilitate the way of people, vehicles, material through doorways of buildings and other enclosures, while eliminating or reducing air transfer, solid doors are replaced or supplemented by air curtains. The air flowing across the doors is induced by the difference of pressure between two rooms generated by the wind or by the ventilation system. Air curtains are popular for energy saving in public buildings, foundry furnaces, refrigeration storages or for air quality control in food, electronic industries and surgical units. Robertson and Shaw (1978) indicate that these devices could also reduce chemical species, odors, bacteria's, dust, insects, moisture or radioactive particles transfer. Grasmuck (1969), Sheikh and Grasmuck (1970), Powlesland (1974) or Partyka (1995) report that this device is also applied for air stopping and flow regulation in mine airways. Another important application is the safety in underground tunnels. In case of fire in gallery, air curtains could reduce the moving of toxic smokes while preserving full access to emergency exits.

The major criterion for the efficiency quantification of an air curtain is the rate of heat and mass transfer crossing it, compared with the same opening without curtain. Robertson and Shaw (1978) have measured the mass transfer with a gas tracer method. The concentration ratio between the protected zone and the polluted one, vary from 5% to 15% when the air curtain correctly seals the

opening. Inversely, if the outlet velocity is too high or the blowing angle not optimal, the air curtain should increase the heat and mass transfer.

The design of air curtains is quite difficult. It depends on the installation site and on the size of the opening. In supermarkets, or public buildings, the velocity must be low to avoid unbearable velocities for pedestrians. For industrial applications, like furnace, refrigeration storage or fire security in tunnel, the velocity may be higher and the jet thicker. Only few recent design data are today available. Actual installations are set up experimentally on scaled down or on expensive full scale models. Nevertheless, we do not have any general correlation at our disposal.

This paper intends to give design information on the air curtain. After some general information on air jets, air curtains designing and fluid mechanics similitude, we give a description of the experimental facilities and methodology. Results on air curtain performances and similitude law are then stated. The most important parameters for design and the limitations in the use of the data obtained on scaled down models are highlighted.

2
Air jet and air curtain description

2.1
Physic of the free air jet

The number of publications involving experimental data, mathematical analysis, and computational modeling points out the importance of air jet in a broad variety of applications. The reviews of Abramovitch (1963), Rajaratnam (1976), Chen and Rodi (1980), Ramaprian and Chandrasekhara (1985) give some piece of information. Depending on the door height, the velocity field of an air jet shows two, three or four regions. We can distinguish the potential core zone, the transition zone, the affinity or developed zone, the impinging or recompression zone. A basic sketch of the velocity distribution of a jet is represented on Fig. 1.

Potential core zone

In this region, the centerline velocity remains constant and equal to the velocity of the jet at exit U_0. The turbulence intensity is also constant. The length of this region is equal to 5 to 8 times the jet thickness e. Van and Howell (1976) indicate that this length is strongly influenced by initial flow conditions and by the shape of the nozzle.

Transition zone

The analytical solution for the velocity distribution of a free jet of low turbulence intensity is given by Eq. (1). It could be applied both to the potential core and to the transition zone. According to Schlichting (1968), the value of the empirical constant σ_1 is equal to 13.5

$$\frac{U(x,y)}{U_0} = \frac{1}{2}\left[1 + \mathrm{erf}\left(\sigma_1 \frac{y + \frac{e}{2}}{x}\right)\right] \quad (1)$$

Affinity or developed zone

This region begins after approximately 20 e. It is also called the affinity region. For a free jet, the velocity field

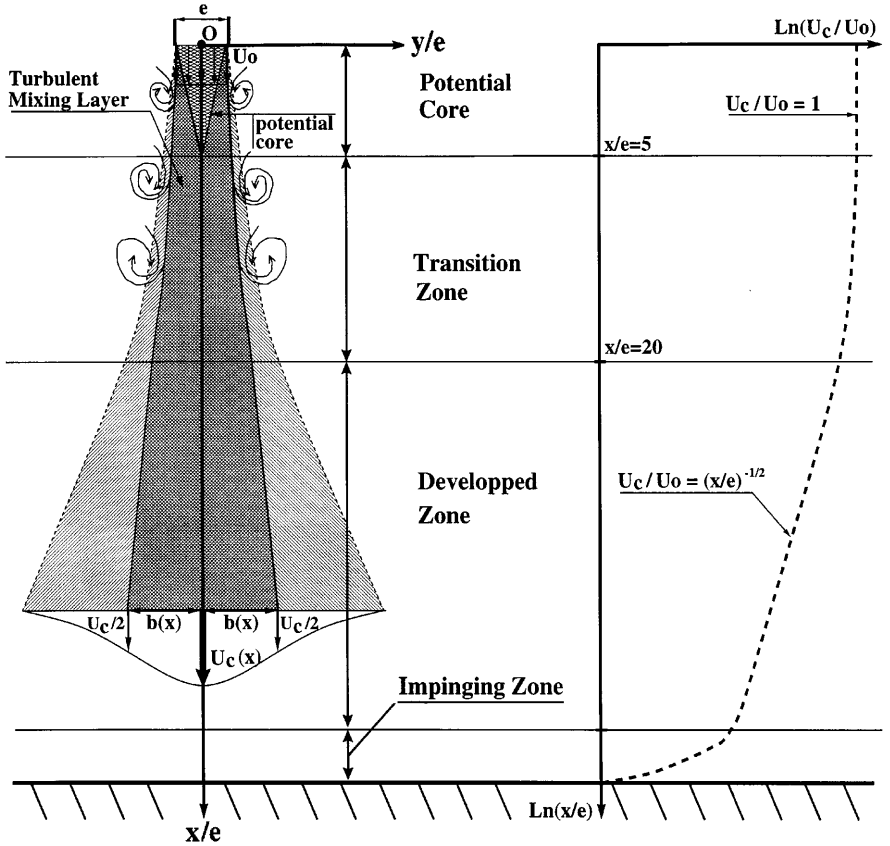

Fig. 1. The different zones of an impinging jet

$U(x,y)$ and the centerline velocity $U_C(x)$ can be respectively calculated by Eqs. (2) and (3), Schlichting (1968):

$$\frac{U(x,y)}{U_0} = \frac{\sqrt{3}}{2}\sqrt{\frac{7.67\,e}{x}}\left[1 - \tanh^2\left(7.67\frac{y}{x}\right)\right] \quad (2)$$

$$\frac{U_C(x)}{U_0} = C_1\left(\frac{x}{e} - C_2\right)^{-\frac{1}{2}} \quad (3)$$

The values of the empirical constants C_1 and C_2, depend on the nozzle shape and on the boundary conditions. They are in the range: $1.9 < C_1 < 3.0$ and $-8 < C_2 < 10$.

Impinging or recompression zone

In air curtain applications, depending on the height of the entrance, only some of the previous regions exist. In all cases, an impinging zone also called the recompression zone is present nearby the floor. The thickness of this zone represents approximately 15% of the total jet height, Gutmark et al. (1978).

2.2 Air curtain theoretical analysis

2.2.1 Dimensional Analysis

Each air curtain installation has specific geometric and dynamic conditions. For a long two dimensional tunnel in the isothermal case, and for an exhaust flow exactly equal to the plane air flow blown at fixed angle α, 8 variables describe the problem: ΔP, H, e, α, U_0, I_0, ν, ρ. Three fundamentally I.S. units (mass, length and time) are involved in the problem. Using the π-Buckingam theorem, we can set up 5 non-dimensional numbers which are representative of the phenomena. There are the geometric aspect ratio H/e, the Reynolds number $U_0\,e/\nu$, the turbulence intensity of the jet I_0 at exit and the blowing angle α. The last number is the ratio of the pressure forces to the inertial forces; it is called the Euler number:
$\mathrm{Eu} = \Delta P/(1/2\rho U_0^2)$. The relationship between these five non-dimensional numbers can be written as following:

$$\frac{\Delta P}{\frac{1}{2}\rho U_0^2} = f\left[\frac{H}{e}, \frac{U_0 e}{\nu}, I_0, \alpha\right] \quad (4)$$

Here is the limit of the dimensional analysis of the problem. The function f must be determined analytically or by means of experiments.

2.2.2 Theoretical calculations of air curtains

To characterize the air curtain efficiency, it is possible to define a minimum discharge velocity U_0, ensuring the sealing of an opening subjected to a cross pressure difference ΔP. The plane air jet closes the door by compensating this pressure difference.

Neglecting the viscous and gravity forces, and considering that the pressure difference is constant along the x-direction, the force budget, in stationary condition, gives the expression of the jet bending. When the transversal mean flow is null, ($U_1 = 0$), the deflection of a jet subjected to a constant transversal pressure difference is an arc of circle of radius R.

$$R = \frac{\rho U_0^2 e}{\Delta P} \quad (5)$$

Using the momentum equation, the integration of the Euler equation gives the expression of the Euler number when the mean flow rate across the air curtain is null.

$$\mathrm{Eu} = k\frac{e}{H}\sin(\alpha) \quad (6)$$

The analytical value of the constant k is equal to 4. Unfortunately, experimental tests done for building energy saving reported by Lajos and Preszler (1975) show that k depends on the ratio H/e; they found for $\alpha = 30°$:

$$k = 1.71 + 0.0264\frac{H}{e} \quad (7)$$

Hayes and Stoecker (1969a, b) have also solved the same problem. Their experiments show that the Euler number depends on the geometric and dynamic parameters of the air curtain. They give an empirical correlation expressing the Euler number as a function of H/e and α:

$$\mathrm{Eu} = 2\frac{e}{H}\left[2.4\sqrt{\frac{e}{H}}\left(1 - 2.56\frac{e}{H}\right) - \sin(\alpha)\right] \quad (8)$$

The main conclusion of their study shows that the Euler number remains constant for each geometric configuration. Thus, for a given entrance, the discharge velocity U_0 of an effective air curtain is proportional to the square root of the pressure difference to be counterbalanced. Experimental works of the previous authors proved the validity of this correlation if $25° < \alpha < 45°$ and $10 < H/e < 40$. Graphic representations of Eqs. (6) and (8) are given on Fig. 2 for $\alpha = 30°$. As only the ratio H/e appears in the correlation, the Euler number seems to be representative of the size of the model. Note that in regard to Eqs. (6)–(8) the value of Euler number does not change when H/e is kept constant. No more details on this topic are given in the papers. Nevertheless, Fig. 2 points out the difference between Lajos and Preszler (1975) and Hayes and Stoecker (1969) results. Experimental conditions seem to have strong effects on results.

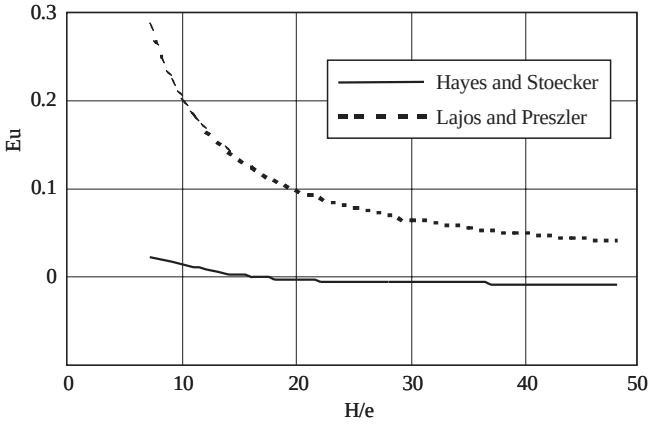

Fig. 2. Experimental correlations suggested by Hayes and Stoecker (1969) and Lajos and Preszler (1975), ($\alpha = 30°$)

More recently, Partyka (1995) analytically solves the problem for mine security application. He has developed a mathematical model yielding data for performance comparison. In this model, a theory for the calculation of the pressure difference created by an air curtain in a rectangular duct is applied to two turbulent plane air streams injected from two opposite walls. His theory can also be applied to an air curtain created by a single jet. Analytical results show that the pressure counterbalanced by the jet is a function of the square of the discharge velocity U_0. The author also picks up that the optimal blowing angle of the jet is closed to 30°. This theory does not fit very well to experimental results. The author proposes to use a correction coefficient varying in the range of 0.35 to 0.9. He does not give more information on this point.

3
Experimental apparatus and procedure

3.1
Test bench description

Figure 3 shows a general view of the installation. The experimental facilities consist of a wind tunnel (1.4 m width, 8 m length) the floor height H of which is adjustable from 0.2 m to 1.44 m. So, the ratio H/e is variable from 12 to 48 for the narrowest nozzle and from 0 to 18 for the broadest one. The air jet blows from top to bottom at a 30° angle to the vertical axis. The maximum velocity is 30 m/s for the narrowest nozzle. The nozzle thickness is 20, 40, 60 or 80 mm. Using a grid, we can set the turbulence intensity of the jet from 0.5% to 20%. The pressure difference on both sides of the air curtain ($P_1 - P_2$) is created with the main tunnel fans. We can set it continually from 0 up to 50 Pa.

3.2
Measurement facilities and experimental procedures

Velocity fields of the air curtain are investigated by a Dantec hot wire anemometer coupled to a micrometric displacement arm. An 8 W laser, and a C.C.D camera are used to visualize the air curtain shape. The pressure differences ($P_1 - P_A$) and ($P_2 - P_1$) are measured in each section with a multichannel pressure sensor of high sensitivity (resolution of 1 Pa). For each section, the static pressures are spatially averaged with eleven parietal taps.

The air curtain is considered fully effective when the pressure difference ($P_1 - P_A$) is null. In that case, the mean mass transfer from the upstream part of the tunnel is null and the flow rate in the downstream part of the tunnel is exactly equal to jet flow rate at exit. This is later called the null mean flow condition.

4
Experimental results

4.1
The free air jet

Before studying the air curtain, we need to verify if the installation is suitable to produce a jet similar to those reported in literature. As shown on Fig. 4, the centerline velocity decay follows the expression given in Eq. (3). The coefficient C_1 is equal to 2.51 and C_2 to 0. They are exactly in the range of values reported by other researchers.

This experimentation also gives the transversal distribution of the jet velocity. Non-dimensional velocity profiles are plotted from x/e = 6 to 50 on Fig. 5. There is a very good agreement with theoretical results given by Rajaratnam (1976). These tests have been conducted for different jet thickness (20 to 80 mm) and several Reynolds

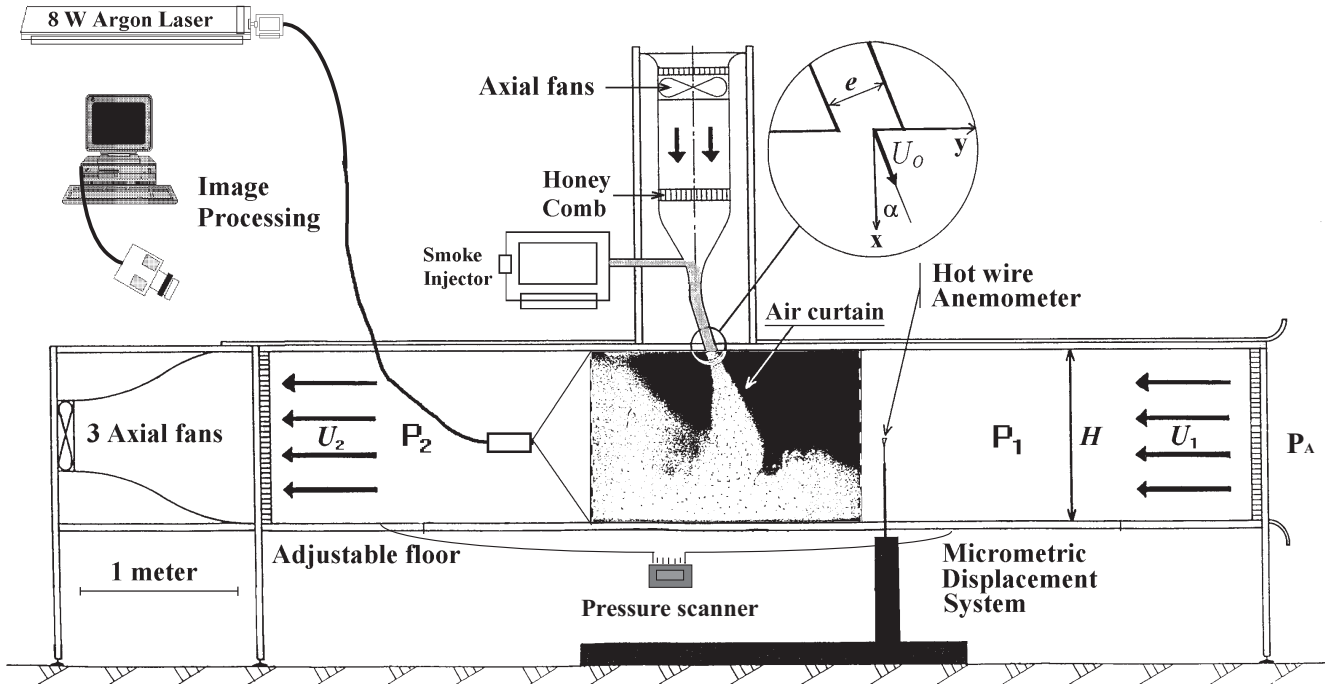

Fig. 3. Schematic view of the installation

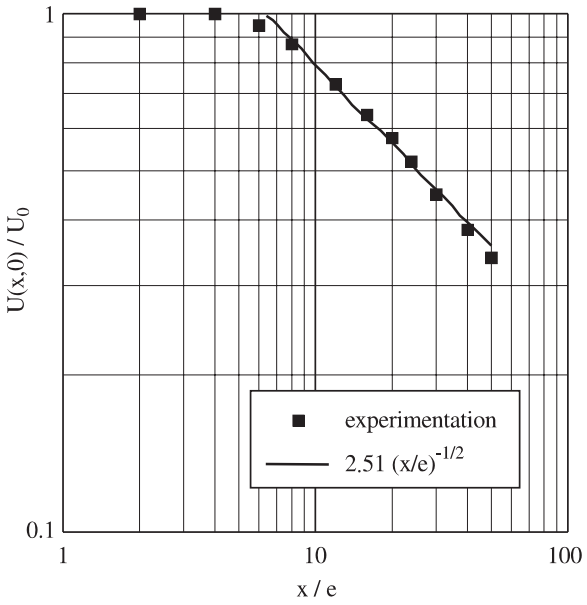

Fig. 4. Centerline velocity decay of a free air jet (U_0 = 27 m/s, I_0 = 0.5%, e = 20 mm, α = 0°)

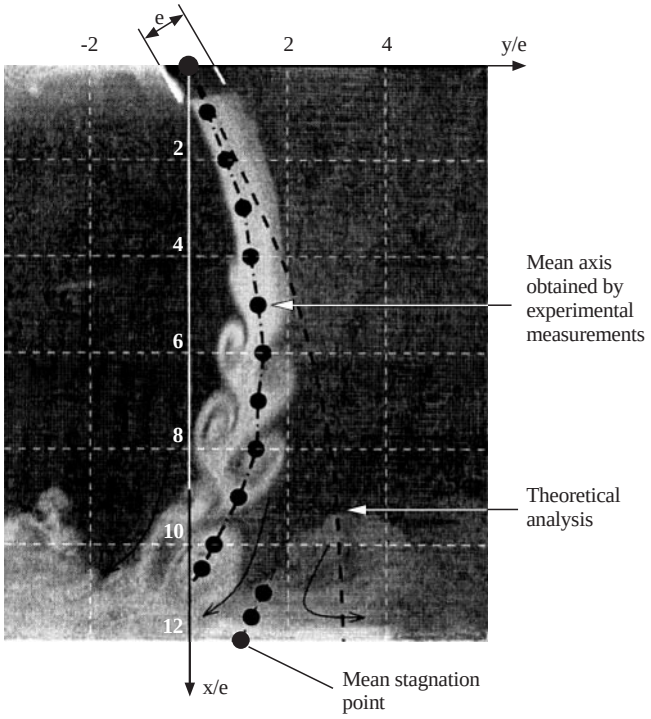

Fig. 6. Laser visualization of the air curtain, theoretical and experimental jet bending at null mean flow condition (U_0 = 3 m/s, I_0 = 0.5%, e = 20 mm, H/e = 12, α = 30°)

number from 33 000 to 66 000. We have obtained the same velocity decays and transversal velocity distributions.

4.2
Shape and curvature of the air curtain

Hayes and Stoecker (1969a, b) and Lajos and Preszler (1975) indicate that the curvature of an air curtain could be approximated by an arc of circle of radius R, Eq. (5). Flow visualizations and centerline velocity measurements done by laser sheet and hot-wire anemometry are shown on Figs. 6 and 7. In case of impingement, the deflection of the jet produced by the pressure difference on both sides cannot be fitted with an arc of circle as promoted by these authors.

Hot-wire anemometry measurements of the velocity field show that the recompression zone interacts on the whole velocity field development. The velocity decay, plotted on Figs. 8 and 9, follows the same law but begins closer to the nozzle. So, theoretical calculations are not adequate for jet bending calculation. In case of a confined jet with impingement closed to the nozzle, Hayes and Stoecker (1969) or Lajos and Preszler (1975) results are not applicable in our case.

4.3
Pressure drop created by the air curtain

Results are presented in form of the pressure difference counterbalanced vs the dynamic pressure of the air jet calculated at exit. It corresponds to the null mean flow condition ($P_1 - P_A = 0$ and $U_1 = 0$). For any given geometry, we observe on Fig. 10, that the Euler number remains constant for each ratio H/e. This result is in good agreement with Hayes and Stoecker (1969a, b) and Lajos

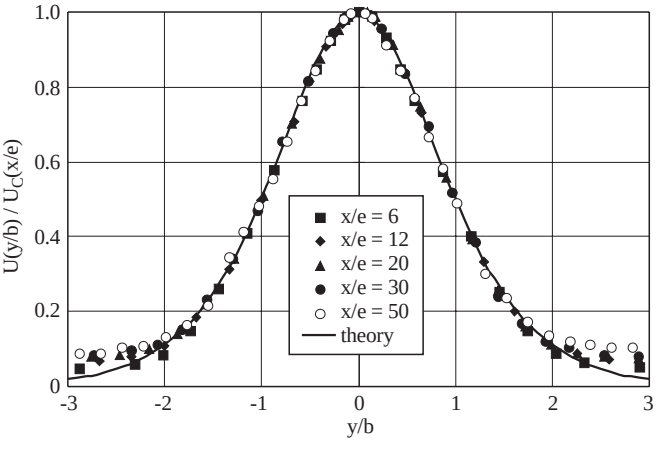

Fig. 5. Dimensionless transversal velocity distribution of a plane air jet (U_0 = 27 m/s, I_0 = 0.5%, e = 20 mm)

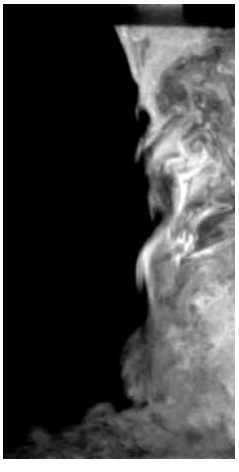

Fig. 7. Visualization of the air curtain frontier (U_0 = 3 m/s, I_0 = 0.5%, e = 20 mm, H/e = 12, α = 30°)

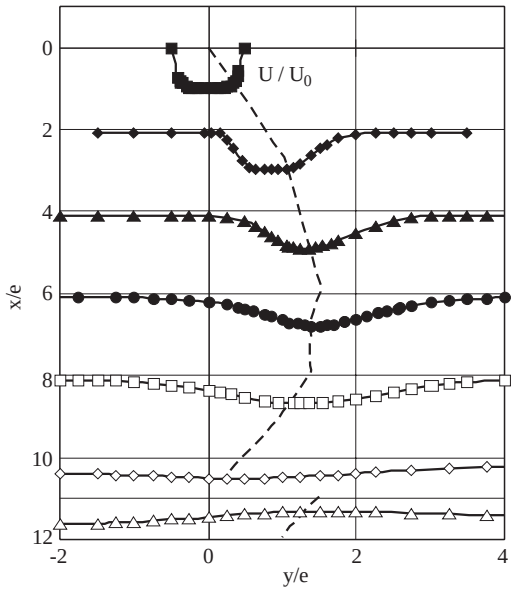

Fig. 8. Velocity distribution of an air curtain (U_0 = 20 m/s, I_0 = 0.5%, e = 20 mm, H/e = 12, α = 30°)

and Preszler (1975) conclusions. We obtain similar results for each air jet thickness (20, 40, 60 and 80 mm).

Therefore, as the slope of the curve remains constant for any given geometry, the Euler number is independent of the Reynolds number of the jet at exit, Re = $U_0 e/\nu$, see Fig. 11. Then, for a study achieved at actual size, we can use the Euler criteria to extrapolate the data. So using the running parameters (U_0; ΔP), we are able to calculate any other setting parameters, for example a higher pressure difference to be counterbalanced.

4.4
Influence of nozzle turbulence intensity

Initial turbulence intensity level I_0 of a jet is usually lower than 2% in laboratory experimentations even though it is

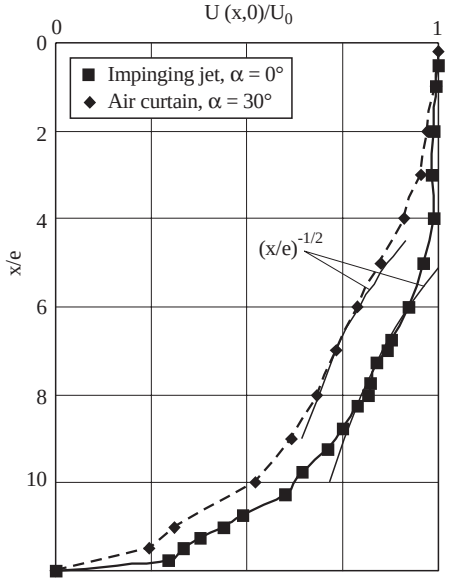

Fig. 9. Centerline velocity decay of a free jet and of an air curtain (U_0 = 20 m/s, I_0 = 0.5%, e = 20 mm, H/e = 12)

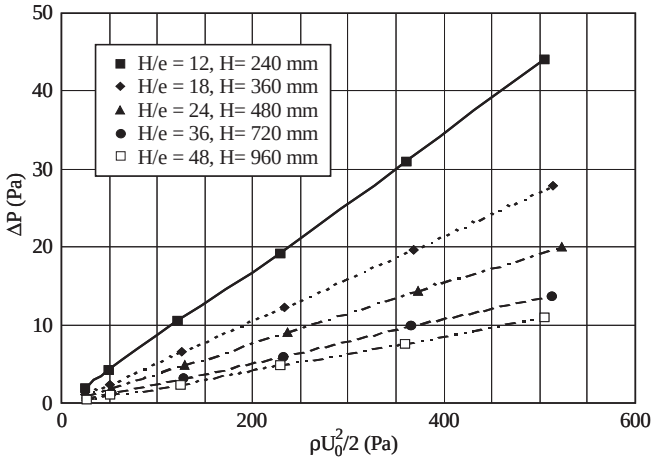

Fig. 10. Pressure difference counterbalanced versus the dynamic pressure of the jet at exit for variable H/e ratio (3 m/s < U_0 < 30 m/s, I_0 = 0.5%, e = 20 mm, α = 30°)

in the range of 10 to 20% in actual air curtains. So it is important to qualify the effect of the turbulence intensity at nozzle on the air curtain performances. Our investigation studies the influence of this parameter on the air screen performances. It appears on Fig. 12, that I_0 does not affect the air curtain performances. The function f in Eq. (4) is independent of I_0. The pressure counter-balanced by the jet is still the same for a fixed air supply velocity and for any turbulence intensity. Only the mean velocity has an effect. This result is of great interest for actual applications because it is very difficult and expensive to keep low the turbulence intensity in such installations.

4.5
Influence of the scale of the model

In many cases, air curtain devices are optimized using geometrically reduced scale models. To verify the accuracy of such model tests, we have changed the scale of the model from 1/4 to 1/1 for a ratio H/e set to 12. Figure 13 shows that the Euler number does not remain constant with the scale changing. Then, it is not correct to use reduced scale models to design air curtain's installations. We effectively show that the Euler number grows with the

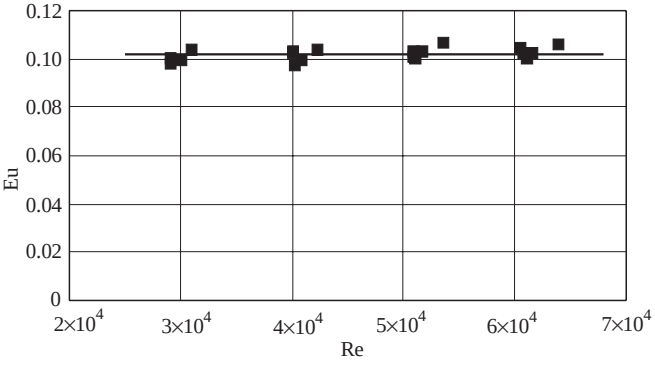

Fig. 11. Euler number versus Reynolds number of the jet at exit (e = 40 mm, H/e = 12, α = 30°)

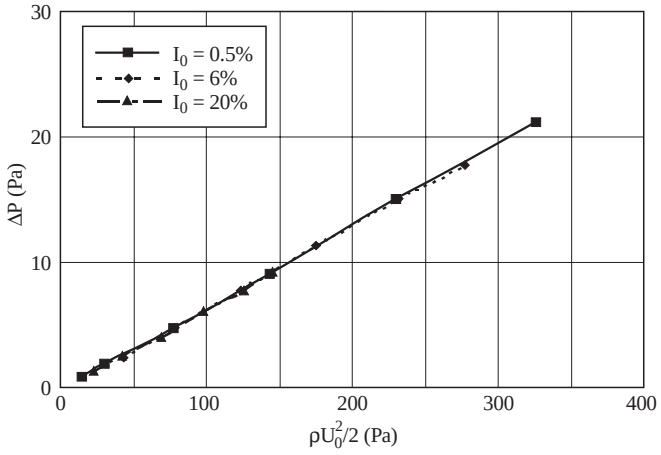

Fig. 12. Pressure difference counterbalanced versus the dynamic pressure of the jet for several jet nozzle turbulence intensities I_0 (3 m/s < U_0 < 30 m/s, I_0 = 0.5%, e = 20 mm, H/e = 12, α = 30°, Eu = 0.07)

device scale. No previous investigations have pointed out this information, neither did Hayes and Stoecker (1969a, b) or Lajos and Preszler (1975).

A constant Euler criteria will give a discharge velocity U_0 stronger than necessary. Then the air curtain creates an opposite flow. In such case, the air curtain can stimulate the fire by provision of fresh air.

4.6
Influence of the ratio *H/e* and *e*

The ratio H/e and the jet thickness e are changed respectively from 20 to 80 mm and from 12 to 48 by floor displacement. On Fig. 14, we plot the curve Eu = $f(H/e,e,\mathrm{Sc})$.

The Euler number does not remain constant with variable geometric conditions (neither with the air curtain scale nor with the ratio H/e).

Nevertheless a semi-empirical correlation has been extracted from our data base:

$$\mathrm{Eu} = \frac{43\,\frac{e}{H}\sqrt{H} - 0.4}{20} \qquad (9)$$

So, there is no available similitude using only the dimensional analysis. Geometric data H, e, jet velocity U_0 and

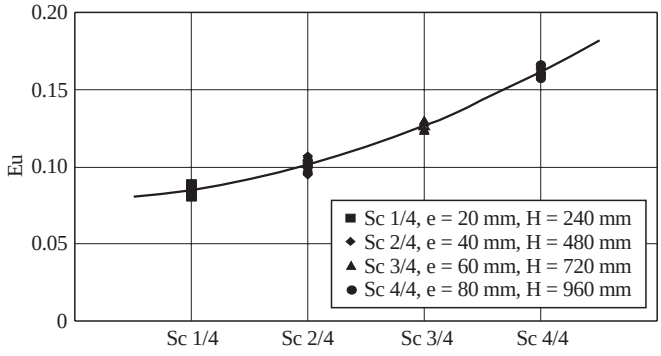

Fig. 13. Variation of the Euler number with the scale of the model (10 m/s < U_0 < 30 m/s, I_0 = 0.5%, H/e = 12, α = 30°)

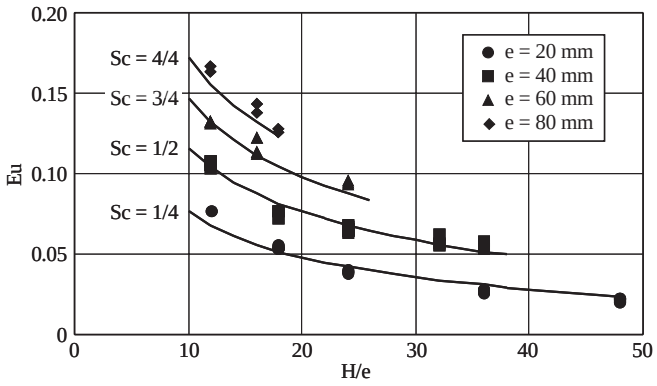

Fig. 14. Euler number as a function of the ratio H/e for different jet thickness (3 m/s < U_0 < 30 m/s, I_0 = 0.5%, α = 30°)

pressure difference are not sufficient to simply describe the fluid mechanics of the air curtain. The convection of the jet vortices, see Guyonnaud et Solliec (1998) and Figs. 6 and 7, and the height of the impinging zone, take part in the air curtain sealing mechanism.

5
Conclusions

According to the former discussion, we cannot give a general correlation apply to the air curtain design. Nevertheless, an extrapolation correlation has been set for an opening from 0.2 to 1.44 m height. Some information of great interest has been pointed out in this study. The main conclusions are the following ones:

- when the pressure difference is increased, the velocity setting of an air curtain can be known with the Euler criteria only if the geometry is unchanged.
- in the range of 0 to 20%, the turbulence intensity does not affect the air curtain performances. Only the mean flow rate is required to ensure the sealing.
- the geometric extrapolation from the reduced scale model using the Euler number similitude is not available. In all cases the Euler extrapolation will give an over-efficient device. In underground applications, the safety will be preserved in all cases. However, care must be taken not to stimulate the fire with opposite flow.

References

Abramovitch GN (1963) The theory of turbulent jets. Massachusetts M.I.T. press

Chen CJ; Rodi W (1980) Vertical buoyant jets. Oxford, Pergamon presses

Grasmuck G (1969) Applicability or air stopping and flow regulators in mine ventilation. C.I.M.M. Bulletin 62: 1175–1185

Gutmark E; Wolfshtein M; Wytganski I (1978) The plane turbulent impinging jet. J Fluid Mech 88: 737–756

Guyonnaud L; Solliec C (1998) Mass transfer analysis of an air curtain system. Advances In Fluid Mechanics, Computational Fluid Mechanics Publications, pp. 139–148

Hayes FC; Stoecker WF (1969a) Heat transfer characteristics of the air curtains. Transaction of the ASHRAE N° 2120: 153–167

Hayes FC; Stoecker WF (1969b) Design data for air curtains. Transactions of the ASHRAE N° 2121: 168–180

Lajos T; Preszler L (1975) Untersuchung von Türluftschleieranlagen. Heizung, Lüftung, Klimatechnick, Haustechnik, Teil 1: 26: 171–176; Teil 2: 26: 226–235
Partyka J (1995) Analytical design of an air curtain. Int J Modelling and Simulation 15: 14–22
Powlesland JW (1974) Air curtains in controlled energy flows. Tunnels and Tunnelling 52–58
Rajaratnam N (1976) Turbulent jets. Elsevier, Amsterdam
Ramaprian BR; Chandrasekhara MS (1985) LDA measurements in plane turbulents jets. J Fluids Eng 107: 264–271
Roberson P; Shaw BH (1978) The linear air curtain as a particulate barrier. J Environ Sci 21: 32–33
Schlichting (1968) Boundary layer theory. Mc Graw-Hill Book, New York
Sheick AM; Grasmuck G (1970) Testing Berry air curtains for stope ventilation of Opemiska. Canadian Mining Canadian Mining J 91(5): 52–55
Van NQ; Howell RH (1976) Influence of initial turbulence intensity on the development of plane air-curtain jets. Transaction of the ASHRAE, n° 2396: 208–228